

Shower angular resolution in IceCube-Gen2 and implications on diffuse science

The IceCube-Gen2 Collaboration

(a complete list of authors can be found at the end of the proceedings)

E-mail: lu.lu@icecube.wisc.edu, maxwell.nakos@icecube.wisc.edu, jvansanten@icecube.wisc.edu, tyuan@icecube.wisc.edu

Over the past decade, the IceCube Neutrino Observatory has discovered a diffuse astrophysical flux and evidence for the first astrophysical neutrino sources, thus highlighting the utility of neutrinos as a new messenger in astronomy. IceCube-Gen2, proposed to be eight times larger than the current detector, will be able to accelerate new discoveries. In order to reach the target volume necessary, the detector is designed with a sparser string spacing. With twice the interstring distance of IceCube, the angular reconstruction of particle showers in IceCube-Gen2 will benefit from new multi-PMT optical modules, accurate modeling of ice properties and a precise understanding of all available sensor data. In this contribution, we show the achievable angular and energy resolutions for shower events observed in IceCube-Gen2 and their dependencies on sensor efficiencies. Implications on diffuse measurements will also be discussed.

Corresponding authors: Lu Lu^{1*}, Maxwell Nakos¹, Jakob van Santen², Tianlu Yuan¹

The 38th International Cosmic Ray Conference (ICRC2023) 26 July – 3 August, 2023 Nagoya, Japan



¹ Dept. of Physics and Wisconsin IceCube Particle Astrophysics Center, University of Wisconsin–Madison

² DESY Zeuthen, Germany

^{*} Presenter

1. Introduction

High-energy neutrinos, originating from cosmological distances, play a crucial role in advancing our understanding of fundamental particle physics and exploring the extreme realms of the Universe. To detect and study these elusive particles, the IceCube Neutrino Observatory was constructed at the geographic South Pole over a decade ago [1]. With its state-of-the-art instrumentation and data collection capabilities, IceCube has provided invaluable insights into the cosmic neutrino landscape. Notably, the IceCube collaboration reported neutrinos emitted from astrophysical sources in close proximity to supermassive black holes, such as NGC 1068 [2], TXS 0506+056 [3, 4], as well as neutrinos originating from within our own galaxy, the Milky Way [5].

In order to improve the detection efficiency for high-energy neutrinos, it is essential to increase the size of the detection volume. As a result, the spacing between strings in the detector has been expanded from 120 m to 240 m [6]. A larger detector also allows better pointing with high-energy muon and tau tracks thanks to a longer lever arm and therefore support point source identifications and multimessenger follow ups [7]. However, the impact of the expanded detector on cascades from charged current electron neutrino interactions and all-flavour neutral current interactions is less certain.

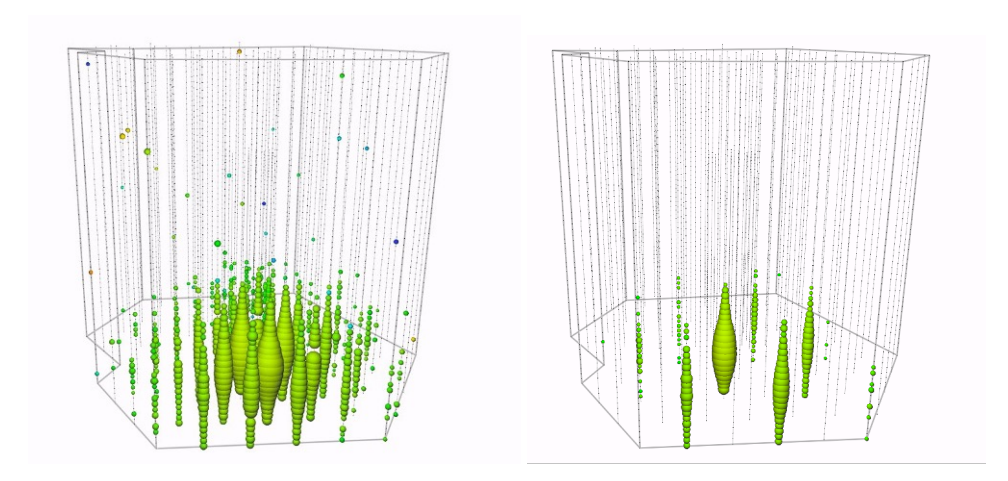


Figure 1: An example 100 TeV electron neutrino induced charged current event seen in IceCube (left) and in Gen2 (right)

Cascades play a critical role in detecting extragalactic and galactic diffuse neutrino emissions. Compared to tracks from muon neutrinos, cascades originating from electron and tau neutrinos possess a distinct advantage due to their reduced probability to the atmospheric neutrino background [8]. Typically, photons produced by a 100 TeV cascade resulting from an electron neutrino-induced shower can travel to strings within a range of ~ 300 m, depending on the optical properties of the ice layer where the interaction takes place [9]. Figure 1 (left) illustrates an event simulation of such a cascade in IceCube, while Fig. 1 (right) shows the corresponding detector response in the context of Gen2.

Accurate angular resolution of cascades is crucial for diffuse analyses. It helps to distinguish the signal from the atmospheric prompt neutrino flux by leveraging the self-veto mechanism [8, 10, 11], which considers the presence of accompanying muons within the same cosmic-ray shower.

Additionally, precise pointing capabilities with cascades are essential for measuring the diffuse flux originating from the Galactic plane and for searching for extended point sources in that region.

In this proceeding, we focus on the idealized angular resolution of cascades in IceCube and IceCube-Gen2, assuming perfect knowledge of the ice and detector properties. Our study is based on the use of single-pixel light sensors. Additionally, we provide a brief discussion on the potential reconstruction improvements that can be achieved by introducing segmented sensors in the ice.

2. Cascade reconstruction

There is a trade-off between speed and accuracy in photon yield models used in reconstruction. For the purposes of this proceeding, we focus on event reconstruction with relatively fast evaluation times at the expense of additional approximations.

Due to sparse instrumentation and complexity inherent in the natural detection medium, several challenges arise in the reconstruction of particle showers. These include ice modeling [12], shower longitudinal extension [13], and randomness introduced by the response of the detector itself [1]. The essence of event reconstruction routines used in IceCube relies on recovering the underlying physics parameters that yield photon arrival time expectations most closely matching the observed data, which can be simulated or real [14]. Likelihood-based metrics to define closeness are widely employed. With such approaches, it is obvious that accurate modeling is important and necessary in order to reduce systematic bias [15, 16]. In this section, we discuss approaches taken to evaluate ideal directional resolution for cascades and potential room for future improvement by incorporating multi-PMT sensors [17, 18].

2.1 Ideal cascade resolution

In order to illustrate the potential of ice as a natural neutrino detector and directly compare shower reconstruction with IceCube-Gen2 to that in IceCube, we use simplified model where contained cascades in IceCube are in addition reconstructed with a Gen2-like string spacing. An example of such an event in both geometries is shown in Fig. 1, and a simulated sample of contained cascades is used for performance evaluation. Furthermore, several assumptions are made in the simulation used for the benchmark. First, we require the ice model used in simulation to exactly match that used in reconstruction. Second, we assume that the cascade longitudinal extension is negligible. Third, we assume a detector response function that does not introduce additional smearing in the conversion of photons incident at the PMT photocathode to the actual digitized data stored as a timeseries of representations of photoelectrons [1]. That is, we assume an idealized version of cascade and detector. These assumptions allow us to set a limit on what is achievable for cascade reconstruction due to only photon statistical fluctuations.

The left panel of Fig. 2 shows the IceCube median angular resolution for a sample of simulated, contained electron (anti)neutrino interactions as a function of the true, deposited energy and obtained under the idealized scenario described above. The blue (orange) solid line shows the median 50% quantile over the distribution in angular spread between true and reconstructed directions when including (excluding) the nearest, "bright", DOMs. The respective color bands correspond to the 25% and 75% quantiles for the angular distance distribution. At an energy of 1 PeV the resolution is below one degree when including bright DOMs. A visual comparison to the event views shown

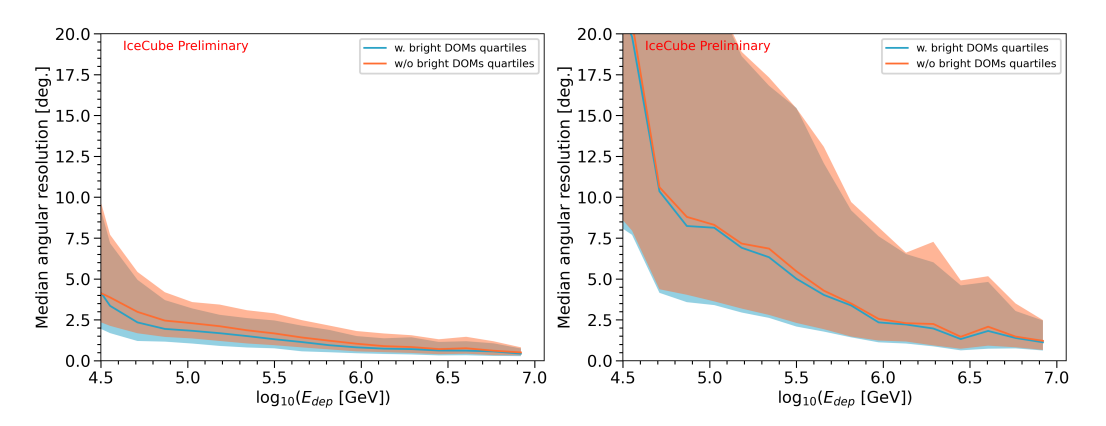


Figure 2: The left panel shows the median angular resolution (solid lines) for an idealized sample of IceCube-contained cascades is shown as a function of the deposited energy. The blue (orange) line shows the resolution with (without) the nearest DOMs, typically referred to as "bright" DOMs. Color bands corresponds to the 25% and 75% quantiles for the angular distance distribution. The right panel shows the same reconstruction with bright DOMs, but for an approximate IceCube Gen2 string spacing. A toy Gen2 geometry is obtained by masking out IceCube strings such that the approximate inter-string distance is doubled compared to IceCube's. The additional photocathode coverage expected for Gen2 DOMs is approximated by a global increased efficiency that is three times the detection efficiency of IceCube DOMs. Thus, this does not incorporate directionality information from multi-PMT sensors, which are under construction for IceCube-Gen2.

in Fig. 1 illustrates the challenge in cascade reconstruction while highlighting the impressiveness of a less than 1° resolution, even if only currently under the idealized scenario.

IceCube-Gen2 is envisioned as a detector approximately eight times larger than IceCube. To stay within resource constraints, Gen2 strings will be spaced approximately 240 m apart. Thus, with roughly double the string spacing of IceCube, the instrumentation in IceCube Gen2 is effectively four times sparser. New sensors planned for Gen2 will have increased photocathode coverage, increasing light detection efficiency by up to a factor of four. However, the light yield falls off exponentially with distance and this limits the absolute photon statistics detectable by Gen2 for cascade-like morphologies [14]. The resolution obtained under the idealized scenario for a toy Gen2 geometry with a global OM efficiency scaling of 3× IceCube-DOM equivalent is shown in Fig. 2 (right panel) and, while there is clear degradation compared to the left panel, it is worth highlighting that at 1 PeV the median resolution is approximately 2.5°. Considering that this is for the reconstruction of particle showers that appear nearly spherical, the potential to utilize cascade directionality in IceCube Gen2 is high if sensor information can be accurately and efficiently unlocked.

2.2 Potential improvements with future multi-pixel sensors

The Long Optical Module (LOM) is a sensor currently being developed for IceCube-Gen2. It combines the elongated shape of the D-Egg (Dual optical sensors in an Ellipsoid Glass for Gen2) with the 4π pixelation of the mDOM (Multi-PMT Digital Optical Module), both of which will be deployed for the IceCube Upgrade [19]. The LOM is the reference optical sensor design for IceCube-Gen2 [20], equipped with either 16 or 18 PMTs per sensor. The LOM design offers a

sensitivity gain of approximately four times the current IceCube DOM and provides additional timing-dependent directional information.

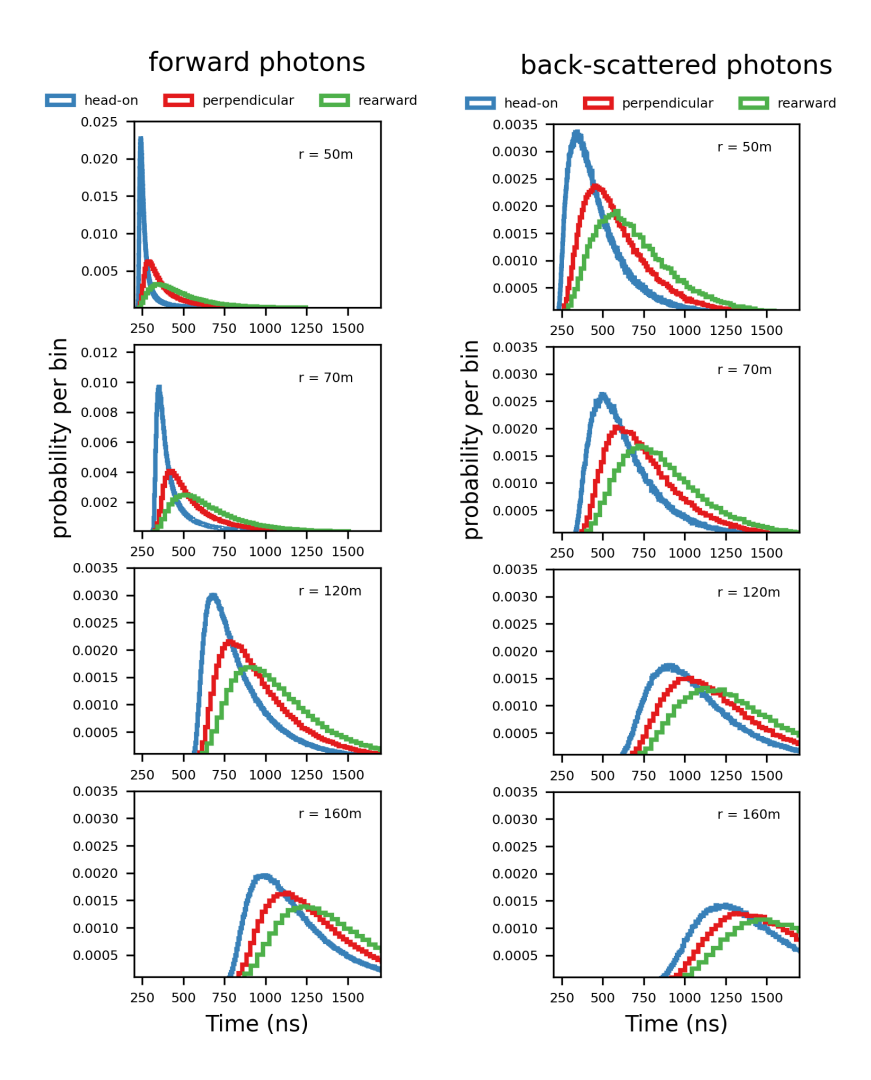


Figure 3: Timing Distributions for Forward (left) and Back-Scattered (right) for Photons emitted in a single direction in homogeneous ice. The forward scattered photons are arriving from the direction of the source. The backwards scattered photons are arriving from the direction away from the source. Head-on photons are when the photons are emitted in the direction of the sensor, perpendicular are when photons are emitted in a direction perpendicular to the sensor, and rearward are when photons are emitted away from the sensor.

The directional reconstruction method for the LOM relies on a maximum likelihood fit, which involves six free parameters: the interaction time, vertex position and the direction angles. When the emission direction of the initial photon changes, the timing distributions at a given sensor location in the ice undergo variations in shape and relative flux. These changes are influenced by factors such as the distance from the source and the arrival direction of the photons.

To illustrate the reconstruction improvement achieved with pixelation, we conducted simulations using an up-going photon emitter [21]. In the simulation, we injected photons with wavelengths sampled from the Cherenkov radiation spectrum, taking into account the wavelength acceptance of the photon sensors [1]. The effective scattering length and the absorption length of the photons

were set to 19.9 m and 63.8 m, respectively. During the simulation, the positions and directions of photons are traced and recorded.

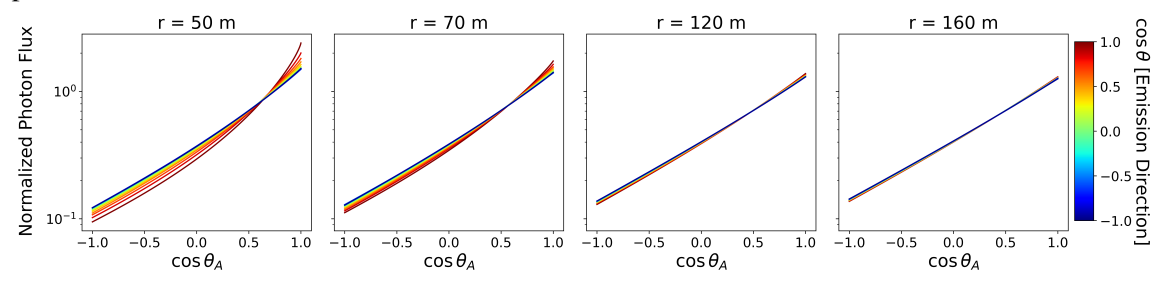


Figure 4: The four panels depict the normalized photon flux as a function of the arrival zenith of the photon $(\cos \theta_A)$ depending on the emission direction of the light source $(\cos \theta)$. The light source is emitting head-on when $\cos \theta$ is 1 and rearward when $\cos \theta$ is -1. The photons are forward scattered when $\cos \theta_A$ is 1 and back-scattered when $\cos \theta_A$ is -1. As distance increases, the shape of the photon arrival flux distribution loses its dependence on emission direction, while the dependence of photon flux on arrival direction remains.

Figure 3 shows directional information of photons emitted in a single direction in homogeneous ice. The forward scattered photons are arriving from the direction of the source. The backwards scattered photons are arriving from the direction away from the source. Head-on photons are when the photons are emitted in the direction of the sensor, perpendicular are when photons are emitted in a direction perpendicular to the sensor, and rearward are when photons are emitted away from the sensor. The risetime of photon arrivals is influenced by various by the position of the receiver relative to the source and the direction of the photons after scatterings [22]. When photons undergo fewer scatterings, the waveform rises more quickly. Figure 4 illustrates the relative photon flux as a function of the photon arrival direction at various distances for different photon emission angles. The figures show that head-on/rearward asymmetries at close distances, which are crucial for providing multi-pixel information for directional reconstruction. Additionally, the forward/backward asymmetry contributes to improved reconstruction of the vertex position, even at a distance of 160 m.

Cascade reconstructions harvesting pixellation information is under development. One notable difference from existing reconstruction algorithms is the inclusion of both the position and directional information of the arrival photons relative to the receiver. Traditionally, only the photon directions are considered, while the positions are marginalized as long as the photons reach the sensor. We expect a further improvement of angular resolution with pixellation taking into account.

3. Implications on diffuse science

The ability to accurately reconstruct the directions of cascades despite the larger detector spacing will substantially improve IceCube-Gen2's ability to observe extended neutrino emission, such as that recently reported from our own galaxy [5]. To illustrate this, we use toise [23] to model IceCube-Gen2's sensitivity to Galactic neutrino emission. To estimate the detector acceptance, we compare the effective area of the selection presented in [24] to a similar selection for IceCube-Gen2, and find that the latter is a factor ~ 8 larger. We take this as a generic scaling factor from IceCube to IceCube-Gen2 for selections of cascade-like events, and apply it to the effective area from [5] to obtain an approximate effective area for a high-acceptance event selection in IceCube-Gen2.

To treat angular resolution, we fit a Fisher-von Mises distribution to the distribution of opening angles for an idealized (but single-pixel) reconstruction in Gen2 (cf. Fig. 2 right panel), and smooth a Galactic emission template in an energy-dependent way using the resulting concentration parameter. Fig. 5 shows examples of this smoothing. In order to be able to compare to existing results in the same framework, we also approximate the response of IceCube using the angular resolution and (unscaled) effective area from [5]. With these approximations, we expect to obtain a median significance of the Galactic emission, assuming that the true flux is $0.55 \times \text{KRA}_{\gamma}^{5}$ (the best fit from [5]), of approximately 11.1σ with 10 years of IceCube-Gen2 data alone, versus approximately 4.7σ for 10 years of IceCube data. In order to demonstrate the high-energy reach of Gen2 for galactic emission, we construct the artificial scenario shown in Fig. 5 (right), where the galactic flux continues with a spectral index of 2.4 beyond the cutoff predicted in the KRA $_{\gamma}^{5}$ model. In this scenario, IceCube would be able to exclude the predicted cutoff with a median significance of only 2.5σ after 10 years of observations, while Gen2 would be able to exclude it with 7.4σ .

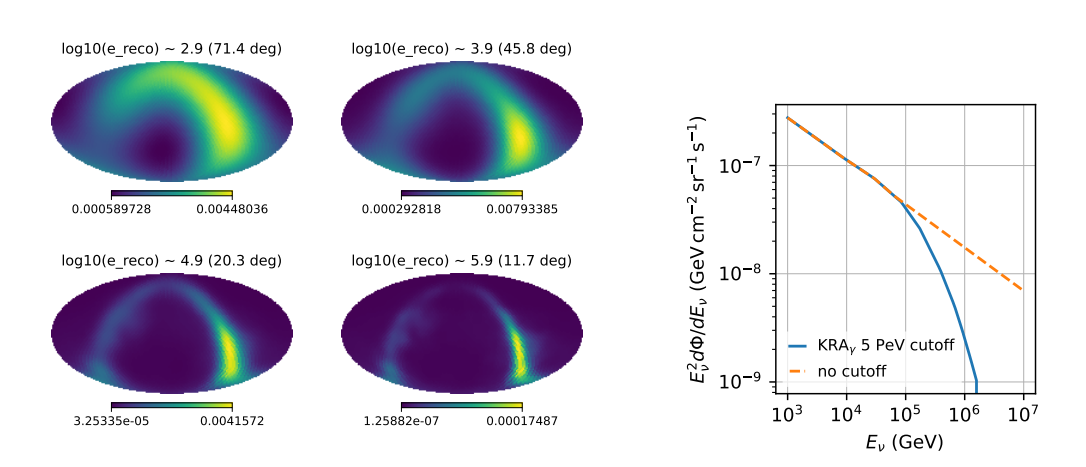


Figure 5: Left: expected distributions of reconstructed galactic neutrino events in Gen2 in four energy bands, assuming the baseline angular resolution shown in Fig. 2 (right panel). The maps are presented in equatorial coordinates with right ascension running left to right from $+180^{\circ}$ to -180° , putting the Galactic center in the lower right of each map. Right: toy flux model to illustrate IceCube-Gen2's ability to distinguish between galactic neutrino emission scenarios. The solid line shows the KRA $_{\gamma}$ flux from [25], scaled to the best-fit normalization found in [5]. The dashed line shows a flux with the same shape at low energies, but that continues beyond the cutoff with a spectral index of 2.4.

4. Conclusion

We presented a simulation study to showcase the idealized angular resolution for cascade events measured in IceCube-Gen2, relying on a sparser version of the IceCube geometry with double the string spacing compared to IceCube. Using a single-pixel sensor with a photon detection efficiency three times that of the IceCube DOM, we achieved a median angular resolution of approximately 8° at 100 TeV and 2.5° at 1 PeV. With such angular resolution and effectively a factor of eight gain of detector volume we expect a rejection of the hypothesis of no cutoff in the diffuse galactic emission at 7.4σ after 10 years of data taking with IceCube-Gen2. Further improvements are expected after taking into account the LOM pixellation information.

References

- [1] IceCube Collaboration, M. G. Aartsen et al. JINST 12 no. 03, (2017) P03012.
- [2] **IceCube** Collaboration, R. Abbasi et al. Science 378 no. 6619, (2022) 538–543.
- [3] **IceCube, Fermi-LAT et al.** Collaboration, M. G. Aartsen *et al. Science* **361** no. 6398, (2018) eaat1378.
- [4] IceCube Collaboration, M. G. Aartsen et al. Science 361 no. 6398, (2018) 147–151.
- [5] **IceCube** Collaboration, R. Abbasi *et al. Science* **380** no. 6652, (2023) 1338–1343.
- [6] IceCube-Gen2 Collaboration, M. G. Aartsen et al. J. Phys. G 48 no. 6, (2021) 060501.
- [7] M. Ackermann et al. JHEAp 36 (2022) 55–110.
- [8] T. K. Gaisser, K. Jero, A. Karle, and J. van Santen Phys. Rev. D 90 no. 2, (2014) 023009.
- [9] IceCube Collaboration, M. G. Aartsen et al. JINST 9 (2014) P03009.
- [10] S. Schonert, T. K. Gaisser, E. Resconi, and O. Schulz *Phys. Rev. D* **79** (2009) 043009.
- [11] C. A. Argüelles, S. Palomares-Ruiz, A. Schneider, L. Wille, and T. Yuan *JCAP* **07** (2018) 047.
- [12] R. Abbasi et al. The Cryosphere Discussions 2022 (2022) 1–48.
- [13] L. Radel and C. Wiebusch Astropart. Phys. 44 (2013) 102–113.
- [14] **IceCube** Collaboration, M. G. Aartsen et al. JINST 9 (2014) P03009.
- [15] IceCube Collaboration, M. Huennefeld et al. PoS ICRC2021 (2021) 1065.
- [16] **IceCube** Collaboration, T. Yuan Nucl. Instrum. Meth. A (2023) 168440.
- [17] **IceCube** Collaboration, Y. Makino *PoS* **ICRC2023** (these proceedings) 979.
- [18] **IceCube** Collaboration, S. Griffin *PoS* **ICRC2023** (these proceedings) 1039.
- [19] **IceCube** Collaboration, A. Ishihara *PoS* **ICRC2019** (2021) 1031.
- [20] **IceCube-Gen2** Collaboration *IceCube-Gen2 Technical Design: The IceCube-Gen2 Neutrino Observatory* https://icecube-gen2.wisc.edu/science/publications/TDR (2023).
- [21] IceCube Collaboration, D. Chirkin Nucl. Instrum. Meth. A 725 (2013) 141–143.
- [22] **AMANDA** Collaboration, J. Ahrens et al. Nucl. Instrum. Meth. A **524** (2004) 169–194.
- [23] J. van Santen, B. A. Clark, R. Halliday, S. Hallmann, and A. Nelles *JINST* 17 no. 08, (2022) T08009.
- [24] IceCube Collaboration, M. G. Aartsen et al. Astrophys. J. 846 no. 2, (2017) 136.
- [25] D. Gaggero, D. Grasso, A. Marinelli, A. Urbano, and M. Valli *The Astrophysical Journal Letters* **815** no. 2, (Dec, 2015) L25.

Full Author List: IceCube-Gen2 Collaboration

R. Abbasi¹⁷, M. Ackermann⁷⁶, J. Adams²², S. K. Agarwalla^{47, 77}, J. A. Aguilar¹², M. Ahlers²⁶, J.M. Alameddine²⁷, N. M. Amin⁵³, K. Andeen⁵⁰, G. Anton³⁰, C. Argüelles¹⁴, Y. Ashida⁶⁴, S. Athanasiadou⁷⁶, J. Audehm¹, S. N. Axani⁵³, X. Bai⁶¹, A. Balagopal V.⁴⁷, M. Baricevic⁴⁷, S. W. Barwick³⁴, V. Basu⁴⁷, R. Bay⁸, J. Becker Tjus^{11, 78}, J. Beise⁷⁴, C. Bellenghi³¹, C. Benning¹, S. BenZvi⁶³, D. Berley²³, E. Bernardini⁵⁹, D. Z. Besson⁴⁰, A. Bishop⁴⁷, E. Blaufuss²³, S. Blot⁷⁶, M. Bohmer³¹, F. Bontempo³⁵, J. Y. Book¹⁴, J. Borowka¹, C. Boscolo Meneguolo⁵⁹, S. Böser⁴⁸, O. Botner⁷⁴, J. Böttcher¹, S. Bouma³⁰, E. Bourbeau²⁶, J. Braun⁴⁷, B. Brinson⁶, J. Brostean-Kaiser⁷⁶, R. T. Burley², R. S. Busse⁵², D. Butterfield⁴⁷, M. A. Campana⁶⁰, K. Carloni¹⁴, E. G. Carnie-Bronca², M. Cataldo³⁰, S. Chattopadhyay^{47, 77}, N. Chau¹², C. Chen⁶, Z. Chen⁶, D. Chirkin⁴⁷, S. Choi⁶⁷, B. A. Clark²³, R. Clark⁴², L. Classen⁵², A. Coleman⁷⁴, G. H. Collin¹⁵, J. M. Conrad¹⁵, D. F. Cowen^{71, 72}, B. Dasgupta⁵¹, P. Dave⁶, C. Deaconu^{20, 21}, C. De Clercq¹³, S. De Kockere¹³, J. DeLaunay⁷⁰, D. Delgado¹⁴, S. Deng¹, K. Deoskar⁶⁵, A. Desai⁴⁷, P. Desiati⁴⁷, K. D. de Vries¹³, G. de Wasseige⁴⁴, T. DeYoung²⁸, A. Diaz¹⁵, J. C. Díaz-Vélez⁴⁷, M. Dittmer⁵², A. Domi³⁰, H. Dujmovic⁴⁷, M. A. DuVernois⁴⁷, T. Ehrhardt⁴⁸, P. Eller³¹, E. Ellinger⁷⁵, S. El Mentawi¹, D. Elsässer²⁷, R. Engel^{35, 36}, H. Erpenbeck⁴⁷, J. Evans²³, J. J. Evans⁴⁹, P. A. Evenson⁵³, K. L. Fan²³, K. Fang⁴⁷, K. Farrag⁴³, K. Farrag¹⁶, A. R. Fazely⁷, A. Fedynitch⁶⁸, N. Feigl¹⁰, S. Fiedlschuster³⁰, C. Finley⁶⁵, L. Fischer⁷⁶, B. Flaggs⁵³, D. Fox⁷¹, A. Franckowiak¹¹, A. Fritz⁴⁸, T. Fujii⁵⁷, P. Fürst¹, J. Gallagher⁴⁶, E. Ganster¹, A. Garcia¹⁴, L. Gerhardt⁹, R. Gernhaeuser³¹, A. Ghadimi⁷⁰, Pranckowiak¹, A. Fritz², 1. Fujii², P. Furst², J. Gainagner¹, E. Ganster², A. Garcia , L. Germatut , R. Germatut , R S. Hickford⁷⁵, A. Hidvegi⁶⁵, J. Hignight²⁹, C. Hill¹⁶, G. C. Hill², K. D. Hoffman²³, B. Hoffmann³⁶, K. Holzapfel³¹, S. Hori⁴⁷, K. Hoshina^{47, 79}, W. Hou³⁵, T. Huber³⁵, T. Huege³⁵, K. Hughes^{19, 21}, K. Hultqvist⁶⁵, M. Hünnefeld²⁷, R. Hussain⁴⁷, K. Hymon²⁷, S. In⁶⁷, A. Ishihara¹⁶, M. Jacquart⁴⁷, O. Janik¹, M. Jansson⁶⁵, G. S. Japaridze⁵, M. Jeong⁶⁷, M. Jin¹⁴, B. J. P. Jones⁴, O. Kalekin³⁰, D. Kang³⁵, W. Kang⁶⁷, X. Kang⁶⁰, A. Kappes⁵², D. Kappesser⁴⁸, L. Kardum²⁷, T. Karg⁷⁶, M. Karl³¹, A. Karle⁴⁷, T. Katori⁴², U. Katz³⁰, M. Kauer⁴⁷, J. L. Kelley⁴⁷, A. Khatee Zathul⁴⁷, A. Kheirandish^{38, 39}, J. Kiryluk⁶⁶, S. R. Klein^{8, 9}, T. Kobayashi⁵⁷, A. Kochocki²⁸, H. Kolanoski¹⁰, T. Kontrimas³¹, L. Köpke⁴⁸, C. Kopper³⁰, D. J. Koskinen²⁶, P. Koundal³⁵, M. Kovacevich⁶⁰, M. Kowalski^{10, 76}, T. Kozynets²⁶, C. B. Krauss²⁹, I. Kravchenko⁴¹, J. Krishnamoorthi^{47, 77}, E. Krupczak²⁸, A. Kumar⁷⁶, E. Kun¹¹, N. Kurahashi⁶⁰, N. Lad⁷⁶, C. Lagunas Gualda⁷⁶, M. J. Larson²³, S. Latseva¹, F. Lauber⁷⁵, J. P. Lazar^{14, 47}, J. W. Lee⁶⁷, K. Leonard DeHolton⁷², A. Leszczyńska⁵³, M. Lincetto¹¹, Q. R. Liu⁴⁷, M. Liubarska²⁹, M. Lohan⁵¹, E. Lohfink⁴⁸, J. LoSecco⁵⁶, C. Love⁶⁰, C. J. Lozano Mariscal⁵², L. Lu⁴⁷, F. Lucarelli³², Y. Lyu^{8, 9}, J. Madsen⁴⁷, K. B. M. Mahn²⁸, Y. Makino⁴⁷, S. Mancina^{47, 59}, S. Mandalia⁴³, W. Marie Sainte⁴⁷, I. C. Mariş¹², S. Marka⁵⁵, Z. Marka⁵⁵, M. Marsee⁷⁰, I. Martinez-Soler¹⁴, R. Maruyama⁵⁴, F. Mayhew²⁸, T. McElroy²⁹, F. McNally⁴⁵, J. V. Mead²⁶, K. Meagher⁴⁷, S. Mechbal⁷⁶, A. Medina²⁵, M. Meier¹⁶, Y. Merckx¹³, L. Merten¹¹, Z. Meyers⁷⁶, J. Micallef²⁸, M. Mikhailova⁴⁰, J. Mitchell⁷, T. Montaruli³², R. W. Moore²⁹, Y. Morii¹⁶, R. Morse⁴⁷, M. Moulai⁴⁷, T. Mukherjee³⁵, R. Naab⁷⁶, R. Nagai 16, M. Nakos 47, A. Narayan 51, U. Naumann 75, J. Necker 76, A. Negi 4, A. Nelles 30, 76, M. Neumann 52, H. Niederhausen 28, M. U. Nisa²⁸, A. Noell¹, A. Novikov⁵³, S. C. Nowicki²⁸, A. Nozdrina⁴⁰, E. Oberla²⁰, ²¹, A. Obertacke Pollmann¹⁶, V. O'Dell⁴⁷, M. Oehler³⁵, B. Oeyen³³, A. Olivas²³, R. Ørsøe³¹, J. Osborn⁴⁷, E. O'Sullivan⁷⁴, L. Papp³¹, N. Park³⁷, G. K. Parker⁴, E. N. Paudel⁵³, L. Paul^{50, 61}, C. Pérez de los Heros⁷⁴, T. C. Petersen²⁶, J. Peterson⁴⁷, S. Philippen¹, S. Pieper⁷⁵, J. L. Pinfold²⁹, A. Pizzuto⁴⁷, I. Plaisier⁷⁶, M. Plum⁶¹, A. Pontén⁷⁴, Y. Popovych⁴⁸, M. Prado Rodriguez⁴⁷, B. Pries²⁸, R. Procter-Murphy²³, G. T. Przybylski⁹, L. Pyras⁷⁶, J. Rack-Helleis⁴⁸, M. Rameez⁵¹, K. Rawlins³, Z. Rechav⁴⁷, A. Rehman⁵³, P. Reichherzer¹¹, G. Renzi¹², E. Resconi³¹, S. Reusch⁷⁶, W. Rhode²⁷, B. Riedel⁴⁷, M. Riegel³⁵, A. Rifaie¹, E. J. Roberts², S. Robertson^{8, 9}, S. Rodan⁶⁷, G. Roellinghoff⁶⁷, M. Rongen³⁰, C. Rott^{64, 67}, T. Ruhe²⁷, D. Ryckbosch³³, I. Safa^{14, 47}, J. Saffer³⁶, D. Salazar-Gallegos²⁸, P. Sampathkumar³⁵, S. E. Sanchez Herrera²⁸, A. Sandrock⁷⁵, P. Sandstrom⁴⁷, M. Santander⁷⁰, S. Sarkar²⁹, S. Sarkar⁵⁸, J. Savelberg¹, P. Savina⁴⁷, M. Schaufel¹, H. Schieler³⁵, S. Schindler³⁰, L. Schlickmann¹, B. Schlüter⁵², F. Schlüter¹², N. Schmeisser⁷⁵, T. Schmidt²³, J. Schneider³⁰, F. G. Schröder^{35, 53}, L. Schumacher³⁰, G. Schwefer¹, S. Sclafani²³, D. Seckel⁵³, M. Seikh⁴⁰, S. Seunarine⁶², M. H. Shaevitz⁵⁵, R. Shah⁶⁰, A. Sharma⁷⁴, S. Shefali³⁶, N. Shimizu¹⁶, M. Silva⁴⁷, B. Skrzypek¹⁴, D. Smith¹⁹, ²¹, B. Smithers⁴, R. Snihur⁴⁷, J. Soedingrekso²⁷, A. Søgaard²⁶, D. Soldin³⁶, P. Soldin¹, G. Sommani¹¹, D. Southall¹⁹, ²¹, C. Spannfellner³¹, G. M. Spiczak⁶², C. Spiering⁷⁶, M. Stamatikos²⁵, T. Stanev⁵³, T. Stezelberger⁹, J. Stoffels¹³, T. Stürwald⁷⁵, T. Stuttard²⁶, G. W. Sullivan²³, I. Taboada⁶, A. Taketa⁶⁹, H. K. M. Tanaka⁶⁹, S. Ter-Antonyan⁷, M. Thiesmeyer¹, W. G. Thompson¹⁴, J. Thwaites⁴⁷, S. Tilav⁵³, K. Tollefson²⁸, C. Tönnis⁶⁷, J. Torres²⁴, ²⁵, S. Toscano¹², D. Tosi⁴⁷, A. Trettin⁷⁶, Y. Tsunesada⁵⁷, C. F. Tung⁶, R. Turcotte³⁵, J. P. Twagirayezu²⁸, B. Ty⁴⁷, M. A. Unland Elorrieta⁵², A. K. Upadhyay^{47, 77}, K. Upshaw⁷, N. Valtonen-Mattila⁷⁴, J. Vandenbroucke⁴⁷, N. van Eijndhoven¹³, D. Vanneroml⁵, J. van Santen⁷⁶, J. Vara⁵², D. Veberic³⁵, J. Veitch-Michaelis⁴⁷, M. Venugopal³⁵, S. Verpoest⁵³, A. Vieregg^{18, 19, 20, 21}, A. Vijai²³, C. Walck⁶⁵, C. Weaver²⁸, P. Weigel¹⁵, A. Weindl³⁵, J. Weldert⁷², C. Welling²¹, C. Wendt⁴⁷, J. Werthebach²⁷, M. Weyrauch³⁵, N. Whitehorn²⁸, C. H. Wiebusch¹, N. Willey²⁸, D. R. Williams⁷⁰, S. Wissel^{71, 72, 73}, L. Witthaus²⁷, A. Wolf¹, M. Wolf³¹, G. Wörner³⁵, G. Wrede³⁰, S. Wren⁴⁹, X. W. Xu⁷, J. P. Yanez²⁹, E. Yildizci⁴⁷, S. Yoshida¹⁶, R. Young⁴⁰, F. Yu¹⁴, S. Yu²⁸, T. Yuan⁴⁷, Z. Zhang⁶⁶, P. Zhelnin¹⁴, S. Zierke¹, M. Zimmerman⁴⁷

¹ III. Physikalisches Institut, RWTH Aachen University, D-52056 Aachen, Germany

² Department of Physics, University of Adelaide, Adelaide, 5005, Australia

³ Dept. of Physics and Astronomy, University of Alaska Anchorage, 3211 Providence Dr., Anchorage, AK 99508, USA

⁴ Dept. of Physics, University of Texas at Arlington, 502 Yates St., Science Hall Rm 108, Box 19059, Arlington, TX 76019, USA

⁵ CTSPS, Clark-Atlanta University, Atlanta, GA 30314, USA

⁶ School of Physics and Center for Relativistic Astrophysics, Georgia Institute of Technology, Atlanta, GA 30332, USA

- ⁷ Dept. of Physics, Southern University, Baton Rouge, LA 70813, USA
- ⁸ Dept. of Physics, University of California, Berkeley, CA 94720, USA
- ⁹ Lawrence Berkeley National Laboratory, Berkeley, CA 94720, USA
- $^{\rm 10}$ Institut für Physik, Humboldt-Universität zu Berlin, D-12489 Berlin, Germany
- ¹¹ Fakultät für Physik & Astronomie, Ruhr-Universität Bochum, D-44780 Bochum, Germany
- ¹² Université Libre de Bruxelles, Science Faculty CP230, B-1050 Brussels, Belgium
- ¹³ Vrije Universiteit Brussel (VUB), Dienst ELEM, B-1050 Brussels, Belgium
- ¹⁴ Department of Physics and Laboratory for Particle Physics and Cosmology, Harvard University, Cambridge, MA 02138, USA
- ¹⁵ Dept. of Physics, Massachusetts Institute of Technology, Cambridge, MA 02139, USA
- ¹⁶ Dept. of Physics and The International Center for Hadron Astrophysics, Chiba University, Chiba 263-8522, Japan
- ¹⁷ Department of Physics, Loyola University Chicago, Chicago, IL 60660, USA
- ¹⁸ Dept. of Astronomy and Astrophysics, University of Chicago, Chicago, IL 60637, USA
- ¹⁹ Dept. of Physics, University of Chicago, Chicago, IL 60637, USA
- ²⁰ Enrico Fermi Institute, University of Chicago, Chicago, IL 60637, USA
- ²¹ Kavli Institute for Cosmological Physics, University of Chicago, Chicago, IL 60637, USA
- ²² Dept. of Physics and Astronomy, University of Canterbury, Private Bag 4800, Christchurch, New Zealand
- ²³ Dept. of Physics, University of Maryland, College Park, MD 20742, USA
- ²⁴ Dept. of Astronomy, Ohio State University, Columbus, OH 43210, USA
- ²⁵ Dept. of Physics and Center for Cosmology and Astro-Particle Physics, Ohio State University, Columbus, OH 43210, USA
- ²⁶ Niels Bohr Institute, University of Copenhagen, DK-2100 Copenhagen, Denmark
- ²⁷ Dept. of Physics, TU Dortmund University, D-44221 Dortmund, Germany
- ²⁸ Dept. of Physics and Astronomy, Michigan State University, East Lansing, MI 48824, USA
- ²⁹ Dept. of Physics, University of Alberta, Edmonton, Alberta, Canada T6G 2E1
- 30 Erlangen Centre for Astroparticle Physics, Friedrich-Alexander-Universität Erlangen-Nürnberg, D-91058 Erlangen, Germany
- 31 Technical University of Munich, TUM School of Natural Sciences, Department of Physics, D-85748 Garching bei München, Germany
- ³² Département de physique nucléaire et corpusculaire, Université de Genève, CH-1211 Genève, Switzerland
- ³³ Dept. of Physics and Astronomy, University of Gent, B-9000 Gent, Belgium
- ³⁴ Dept. of Physics and Astronomy, University of California, Irvine, CA 92697, USA
- ³⁵ Karlsruhe Institute of Technology, Institute for Astroparticle Physics, D-76021 Karlsruhe, Germany
- ³⁶ Karlsruhe Institute of Technology, Institute of Experimental Particle Physics, D-76021 Karlsruhe, Germany
- ³⁷ Dept. of Physics, Engineering Physics, and Astronomy, Queen's University, Kingston, ON K7L 3N6, Canada
- ³⁸ Department of Physics & Astronomy, University of Nevada, Las Vegas, NV, 89154, USA
- ³⁹ Nevada Center for Astrophysics, University of Nevada, Las Vegas, NV 89154, USA
- ⁴⁰ Dept. of Physics and Astronomy, University of Kansas, Lawrence, KS 66045, USA
- ⁴¹ Dept. of Physics and Astronomy, University of Nebraska-Lincoln, Lincoln, Nebraska 68588, USA
- ⁴² Dept. of Physics, King's College London, London WC2R 2LS, United Kingdom
- ⁴³ School of Physics and Astronomy, Queen Mary University of London, London E1 4NS, United Kingdom
- ⁴⁴ Centre for Cosmology, Particle Physics and Phenomenology CP3, Université catholique de Louvain, Louvain-la-Neuve, Belgium
- ⁴⁵ Department of Physics, Mercer University, Macon, GA 31207-0001, USA
- ⁴⁶ Dept. of Astronomy, University of Wisconsin-Madison, Madison, WI 53706, USA
- ⁴⁷ Dept. of Physics and Wisconsin IceCube Particle Astrophysics Center, University of Wisconsin–Madison, Madison, WI 53706, USA
- ⁴⁸ Institute of Physics, University of Mainz, Staudinger Weg 7, D-55099 Mainz, Germany
- ⁴⁹ School of Physics and Astronomy, The University of Manchester, Oxford Road, Manchester, M13 9PL, United Kingdom
- ⁵⁰ Department of Physics, Marquette University, Milwaukee, WI, 53201, USA
- ⁵¹ Dept. of High Energy Physics, Tata Institute of Fundamental Research, Colaba, Mumbai 400 005, India
- ⁵² Institut für Kernphysik, Westfälische Wilhelms-Universität Münster, D-48149 Münster, Germany
- ⁵³ Bartol Research Institute and Dept. of Physics and Astronomy, University of Delaware, Newark, DE 19716, USA
- ⁵⁴ Dept. of Physics, Yale University, New Haven, CT 06520, USA
- ⁵⁵ Columbia Astrophysics and Nevis Laboratories, Columbia University, New York, NY 10027, USA
- ⁵⁶ Dept. of Physics, University of Notre Dame du Lac, 225 Nieuwland Science Hall, Notre Dame, IN 46556-5670, USA
- ⁵⁷ Graduate School of Science and NITEP, Osaka Metropolitan University, Osaka 558-8585, Japan
- ⁵⁸ Dept. of Physics, University of Oxford, Parks Road, Oxford OX1 3PU, United Kingdom
- ⁵⁹ Dipartimento di Fisica e Astronomia Galileo Galilei, Università Degli Studi di Padova, 35122 Padova PD, Italy
- ⁶⁰ Dept. of Physics, Drexel University, 3141 Chestnut Street, Philadelphia, PA 19104, USA
- ⁶¹ Physics Department, South Dakota School of Mines and Technology, Rapid City, SD 57701, USA
- ⁶² Dept. of Physics, University of Wisconsin, River Falls, WI 54022, USA
- ⁶³ Dept. of Physics and Astronomy, University of Rochester, Rochester, NY 14627, USA
- ⁶⁴ Department of Physics and Astronomy, University of Utah, Salt Lake City, UT 84112, USA
- ⁶⁵ Oskar Klein Centre and Dept. of Physics, Stockholm University, SE-10691 Stockholm, Sweden
- ⁶⁶ Dept. of Physics and Astronomy, Stony Brook University, Stony Brook, NY 11794-3800, USA
- ⁶⁷ Dept. of Physics, Sungkyunkwan University, Suwon 16419, Korea

- ⁶⁸ Institute of Physics, Academia Sinica, Taipei, 11529, Taiwan
- ⁶⁹ Earthquake Research Institute, University of Tokyo, Bunkyo, Tokyo 113-0032, Japan
- ⁷⁰ Dept. of Physics and Astronomy, University of Alabama, Tuscaloosa, AL 35487, USA
- 71 Dept. of Astronomy and Astrophysics, Pennsylvania State University, University Park, PA 16802, USA
- ⁷² Dept. of Physics, Pennsylvania State University, University Park, PA 16802, USA
- ⁷³ Institute of Gravitation and the Cosmos, Center for Multi-Messenger Astrophysics, Pennsylvania State University, University Park, PA 16802, USA
- ⁷⁴ Dept. of Physics and Astronomy, Uppsala University, Box 516, S-75120 Uppsala, Sweden
- ⁷⁵ Dept. of Physics, University of Wuppertal, D-42119 Wuppertal, Germany
- ⁷⁶ Deutsches Elektronen-Synchrotron DESY, Platanenallee 6, 15738 Zeuthen, Germany
- ⁷⁷ Institute of Physics, Sachivalaya Marg, Sainik School Post, Bhubaneswar 751005, India
- ⁷⁸ Department of Space, Earth and Environment, Chalmers University of Technology, 412 96 Gothenburg, Sweden
- ⁷⁹ Earthquake Research Institute, University of Tokyo, Bunkyo, Tokyo 113-0032, Japan

Acknowledgements

The authors gratefully acknowledge the support from the following agencies and institutions: USA - U.S. National Science Foundation-Office of Polar Programs, U.S. National Science Foundation-Physics Division, U.S. National Science Foundation-EPSCoR, Wisconsin Alumni Research Foundation, Center for High Throughput Computing (CHTC) at the University of Wisconsin-Madison, Open Science Grid (OSG), Advanced Cyberinfrastructure Coordination Ecosystem: Services & Support (ACCESS), Frontera computing project at the Texas Advanced Computing Center, U.S. Department of Energy-National Energy Research Scientific Computing Center, Particle astrophysics research computing center at the University of Maryland, Institute for Cyber-Enabled Research at Michigan State University, and Astroparticle physics computational facility at Marquette University; Belgium - Funds for Scientific Research (FRS-FNRS and FWO), FWO Odysseus and Big Science programmes, and Belgian Federal Science Policy Office (Belspo); Germany - Bundesministerium für Bildung und Forschung (BMBF), Deutsche Forschungsgemeinschaft (DFG), Helmholtz Alliance for Astroparticle Physics (HAP), Initiative and Networking Fund of the Helmholtz Association, Deutsches Elektronen Synchrotron (DESY), and High Performance Computing cluster of the RWTH Aachen; Sweden - Swedish Research Council, Swedish Polar Research Secretariat, Swedish National Infrastructure for Computing (SNIC), and Knut and Alice Wallenberg Foundation; European Union - EGI Advanced Computing for research; Australia - Australian Research Council; Canada - Natural Sciences and Engineering Research Council of Canada, Calcul Québec, Compute Ontario, Canada Foundation for Innovation, WestGrid, and Compute Canada; Denmark - Villum Fonden, Carlsberg Foundation, and European Commission; New Zealand - Marsden Fund; Japan - Japan Society for Promotion of Science (JSPS) and Institute for Global Prominent Research (IGPR) of Chiba University; Korea - National Research Foundation of Korea (NRF); Switzerland - Swiss National Science Foundation (SNSF); United Kingdom - Department of Physics, University of Oxford.